Nonlinear properties of lead zirconate–titanate piezoceramics

Wenhua Jiang
Materials Research Laboratory, The Pennsylvania State University, University Park, Pennsylvania 16802

Wenwu Cao[a)]
Department of Mathematics, Materials Research Laboraotry, The Pennsylvania State University, University Park, Pennsylvania 16802

(Received 6 July 2000; accepted for publication 22 September 2000)

Nonlinear properties of lead zirconate-titanate (PZT) piezoceramics are investigated using ultrasonic second harmonic generation technique. When a sinusoidal ultrasonic wave of frequency ω_0 is sent into a nonlinear material, the second harmonic wave with frequency $2\omega_0$ is generated. Through measuring the absolute amplitude of the fundamental (ω_0) and of the second harmonic ($2\omega_0$) waves, the ultrasonic nonlinearity parameter β can be determined, which involves certain combinations of the third-order elastic constants and piezoelectric coefficients. We report the measured nonlinear parameters for four types of doped PZT ceramics, PZT-4, PZT-5A, PZT-5H, and PZT-5H HD, which are widely used in practice. We found that the nonlinear parameter is much more sensitive than the linear parameter in responding to microstructural changes in piezoceramics. It could be used to distinguish unpoled samples from depoled samples, which are undistinguishable in terms of the linear parameters. © *2000 American Institute of Physics.* [S0021-8979(01)02001-1]

I. INTRODUCTION

The lead zirconate–titanate (PZT) ceramics are widely used in ultrasonic transducers, resonators, sensors, ultrasonic motors, actuators, and many other electromechanical devices. Although their linear material properties have been well characterized, little has been reported on their nonlinear elastic properties. The knowledge on the nonlinear elastic properties of PZT materials is very important for devices operating at high field levels, such as many increasingly popular miniaturized piezoelectric devices, which are being driven way out of the linear regime. Under high field, nonlinear effects will have strong impact on device operations and must be taken into account, including frequency-amplitude effect, acoustic power saturation, waveform distortion, and higher harmonic generation. These nonlinear effects can greatly degrade the performance of many electromechanical devices if not being handled carefully. On the other hand, nonlinear acoustic signal processing devices[1] and ultrasonic imaging techniques can employ nonlinear effects as an advantage.

Literature concerning the nonlinear elastic properties of PZT piezoceramics is scarce. Beige measured the nonlinear elastic compliance s_{333}^E and the nonlinear dielectric coefficient ϵ_{333}^T as well as their temperature dependence for modified lead zirconate–titanate ceramics (type Piezolan S_2, L, T_m), by means of resonance method.[2] It was found that the nonlinear coefficients depend strongly on the microstructures of the materials. Na and Breazeale reported the third-order elastic constants c_{111}^E and c_{333}^D of PZT ceramics types K1 and S1 by means of ultrasonic second harmonic generation technique.[3] They reported that the nonlinear coefficients could change several orders of magnitude when the temperature varies from room temperature to temperatures above the Curie temperature.

Our present work is devoted to study the nonlinear properties of the popular PZT ceramics, PZT-4, PZT-5A, conventional PZT-5H (Valpey–Fisher, 75 South St. Hopkinton, MA 01748), and high density PZT-5H HD (Motorola) at room temperature. By means of the ultrasonic second harmonic generation technique, the third-order elastic constants c_{111}^E and c_{333}^D for poled samples and c_{111} for the unpoled and depoled samples are measured. Distinctive nonlinear coefficients were found among these samples.

This article is structured as the following: In Sec. II, a general description will be given to discuss the propagation of ultrasonic waves in poled nonlinear piezoelectric ceramics; in Sec. III the experimental setup and method are described; Sec. IV reports the experimental results together with brief discussions; and Sec. V gives the summary and conclusions.

II. ULTRASONIC SECOND HARMONIC GENERATION IN A PIEZOELECTRIC MATERIAL

Although most materials are assumed to be linear, solid materials are inherently nonlinear, and these nonlinearities will cause anharmonic effects. It was found that ignoring anharmonic terms of phonon vibrations could result in failure of the interpretation of many static and transport properties of solids, such as thermal expansion, temperature dependence of elastic constants, and thermal conductivity.[4] Owing to the anharmonicity, stored energy expansion of a piezoelectric crystal in terms of the elastic strain and the electric field will deviate from a parabolic formulation. Consequently, linear piezoelectricity and elasticity must be modi-

a)Electronic mail: cao@math.psu.edu

fied, particularly at high field and strain levels. When the energy expansion includes cubic terms of the strain and electric field, bilinear constitutive relations, and bilinear electroacoustic equations are obtained. For such a nonlinear medium, if an initially sinusoidal ultrasonic wave of finite amplitude propagates through it, the waveform will be distorted and a second harmonic wave will be generated.

McMahon had discussed ultrasonic second harmonic generation in piezoelectric crystals with $3m$ symmetry,[5] and Nelson had provided a description for three-field interactions in more general dielectric materials.[6] It can be verified that the quasistatic bilinear electromechanical equations can be written, in terms of the material coordinates, as:

$$\rho_0 \ddot{u}_i = (P_{ij}^L + P_{ij}^{\mathrm{NL}})_{,j} \quad (i,j=1,2,3), \tag{1a}$$

$$D_{k,k}^L + D_{k,k}^{\mathrm{NL}} = 0 \quad (i,j=1,2,3). \tag{1b}$$

Here the bilinear constitutive relations are

$$P_{ij} = P_{ij}^L + P_{ij}^{\mathrm{NL}} = c_{ijkl}^E u_{k,l} - e_{kij} E_k + \tfrac{1}{2}(c_{ijklmn}^E + \delta_{ik} c_{ljmn}^E + \delta_{im} c_{njkl}^E + \delta_{km} c_{ijln}^E) u_{k,l} u_{m,n} - (e_{kijmn} + \delta_{im} e_{knj}) u_{m,n} E_k - \tfrac{1}{2} m_{klij} E_k E_l, \tag{2b}$$

$$D_k = D_k^L + D_k^{\mathrm{NL}} = \epsilon_{kl} E_l + e_{klm} u_{l,m} + \tfrac{1}{2}(e_{klmij} + \delta_{li} e_{kmj}) \times u_{l,m} u_{i,j} + m_{klmn} E_l u_{m,n} + \epsilon_{klm} E_l E_m. \tag{2d}$$

The relation of finite strain η_{ij} and particle displacement gradient $\eta_{ij} = \frac{1}{2}(u_{i,j} + u_{j,i} + u_{k,i} u_{k,j})$ is employed in deriving the equations. In Eqs. (1) and (2) the dot above a letter stands for material time derivative, the indices after the comma in the subscript stand for material spatial derivatives, δ_{ij} is the Kronecker delta, P_{ij} is the Piola–Chirhhoff stress tensor, D_k is material electric displacement, ρ_0 is the mass density of the material in unstrained state, c_{ijkl}, e_{ijk}, and ϵ_{ij} are the second-order elastic constants, piezoelectric coefficients and dielectric constants, c_{ijklmn}, e_{ijklm}, and ϵ_{ijk} are the third-order elastic constants, nonlinear piezoelectric coefficients and nonlinear dielectric constants, and m_{ijkl} are the electrostriction constants.

Generally speaking, Eq. (1) can be solved subject to appropriate boundary conditions for any wave propagation direction in the crystal. Here we are only interested in those pure-mode longitudinal waves, which we have also measured experimentally. These longitudinal waves will couple to the piezoelectric effect if the particle displacement direction coincides with the polarization direction. For an anisotropic crystal, the directions allowing pure mode longitudinal wave to propagate are limited.[7] Poled PZT ceramics have a conic ∞m symmetry, which can be treated as $6mm$ symmetry while deriving the differential equations. Pure longitudinal modes exist in the X_3 and X_1 directions (X_3 is the poling direction) for such systems.[7] The longitudinal wave propagating along X_1 does not couple to the piezoelectric effect. Hence, its nonlinear behavior can be described by the equations developed for the nonpiezoelectric solid medium.[8] The longitudinal wave along the X_3 direction is a piezoelectric stiffened wave, and the piezoelectric and dielectric nonlinearities will also contribute to the ultrasonic second harmonic wave generation,[5] which results in effective nonlinear constants as defined below.

For a pure-mode longitudinal wave along X_3, Eq. (1) can be simplified to:

$$\rho_0 \ddot{u}_3 = P_{33,3}, \tag{3a}$$

$$D_{3,3} = 0, \tag{3b}$$

where

$$P_{33} = c_{33}^E u_{3,3} - e_{33} E_3 + \tfrac{1}{2}(c_{333}^E + 3c_{33}^E) u_{3,3}^2 - \tfrac{1}{2} m_{33} E_3^2 - (e_{33} + e_{333}) u_{3,3} E_3, \tag{4a}$$

$$D_3 = \epsilon_{33} E_3 + e_{33} u_{3,3} + \tfrac{1}{2} \epsilon_{333} E_3^2 + m_{33} E_3 u_{3,3} + \tfrac{1}{2}(e_{33} + e_{333}) u_{3,3}^2. \tag{4b}$$

Substituting Eq. (4) into (3) yields

$$\rho_0 \ddot{u}_3 = c_{33}^E u_{3,33} - e_{33} E_{3,3} + (c_{333}^E + 3c_{33}^E) u_{3,3} u_{3,33} - m_{33} E_3 E_{3,3} - (e_{33} + e_{333})(u_{3,3} E_{3,3} + u_{3,33} E_3), \tag{5a}$$

$$\epsilon_{33} E_{3,3} + e_{33} u_{3,33} + \epsilon_{333} E_3 E_{3,3} + m_{33}(E_{3,3} u_{3,3} + E_3 u_{3,33}) + (e_{33} + e_{333}) u_{3,3} u_{3,33} = 0. \tag{5b}$$

Because the nonlinear effect is generally much smaller compared to the linear effect, it may be considered as a perturbation to the linear effects and we can use the successive approximation technique to solve Eq. (5). Let us assume

$$u_3 = \lambda u_3^{(0)} + \lambda^2 u_3^{(1)} + \ldots, \tag{6a}$$

$$E_3 = \lambda E_3^{(0)} + \lambda^2 E_3^{(1)} + \ldots, \tag{6b}$$

where λ is a parameter less than one, which indicates the order of magnitude of the successive terms in Eq. (6). The terms higher than λ^2 are ignored since we only deal with the quadratic nonlinearity and the third order nonlinear constants. Substituting Eq. (6) into Eq. (5) and equating the terms of the same order in λ, we can obtain, respectively, the equations for different orders of the successive approximations in Eq. (6). Among them the first order correction equation for a piezoelectric stiffened longitudinal wave can be written as:

$$\rho_0 \ddot{u}_3^{(1)} - K_2 u_{3,33}^{(1)} = (K_3 + 3K_2) u_{3,3}^{(0)} u_{3,33}^{(0)}. \tag{7}$$

Equation (7) has the same form as that of the nonpiezoelectric longitudinal wave[8] except the second order coefficient K_2 has been redefined as

$$K_2 = c_{33}^D = c_{33}^E + \frac{e_{33}^2}{\epsilon_{33}}, \tag{8}$$

and the third order coefficient K_3 is redefined as

$$K_3 = c_{333}^D = c_{333}^E + \epsilon_{333}\left(\frac{e_{33}}{\epsilon_{33}}\right)^3 - 3m_{33}\left(\frac{e_{33}}{\epsilon_{33}}\right)^2 + 3e_{333}\left(\frac{e_{33}}{\epsilon_{33}}\right). \tag{9}$$

Since the zeroth order equation is simply the linear piezoelectric stiffened wave equation, u_3^0 has the general wave solution:

$$u_3^{(0)} = A_1 \sin(\omega t - kz). \tag{10}$$

Here z is the coordinate along the wave propagation direction. Substituting Eq. (10) into Eq. (7) leads to the second harmonic solution:

$$u_3^{(1)} = A_2 \cos 2(\omega t - kz) = \tfrac{1}{8}\beta k^2 z A_1^2 \cos 2(\omega t - kz), \tag{11}$$

which is the first order correction to the linear solution. The solution (11) satisfies the boundary condition $u_3^{(1)}=0$ at $z=0$. In Eqs. (10) and (11), A_1 and A_2 are amplitudes of the fundamental and second harmonic waves, respectively, ω is the angular frequency, $k=(\omega/v)$ is the wave number and v is the wave velocity given by

$$v = \sqrt{\frac{K_2}{\rho_0}}, \tag{12}$$

β is the nonlinearity parameter defined as

$$\beta = -\frac{3K_2 + K_3}{K_2}. \tag{13}$$

It can be seen from Eq. (11) that the amplitude of the second harmonic wave (degree of waveform distortion for the traveling wave) is proportional to β, which is directly related to Gruneisen parameter of materials[8] and is a measure of the material nonlinearity.

III. EXPERIMENTAL DETERMINATION OF NONLINEARITY PARAMETER β

From Eq. (11), if the amplitudes of the fundamental and the second harmonic waves A_1 and A_2 are known, the nonlinearity parameter β can be calculated from the formula:

$$\beta = \frac{8}{k^2 L}\frac{A_2}{A_1^2}, \tag{14}$$

where L is the distance of wave propagation or sample length. Once the β is determined, K_3 can be calculated from Eq. (13) since K_2 has been measured. Generally speaking, K_2 and K_3 are associated with different combinations of the second- and third-order elastic constants, respectively. For different wave propagation directions in PZT materials, K_2 and K_3 are listed in Table I. Note: poled PZT ceramic has a conic symmetry of ∞m, which is equivalent to a 6*mm* system when calculating the independent elastic constants,[9] while the unpoled and depoled PZT ceramic have isotropic symmetry so that K_2 and K_3 in Table I are equal to c_{11} and c_{111}, respectively.

TABLE I. Directions allowing pure mode longitudinal wave and the corresponding second- and third-order elastic constants of materials with 6*mm* and ∞m symmetries.

K parameters	Z direction	X direction[a]
K_2	c_{33}^D	c_{11}^E
K_3	c_{333}^D	c_{111}^E

[a]For isotropic materials (e.g., unpoled and depoled PZT ceramics), there is no difference between the elastic constants under constant electric displacement **D** and constant electric field **E**, the superscript E is therefore ignored in most literatures.

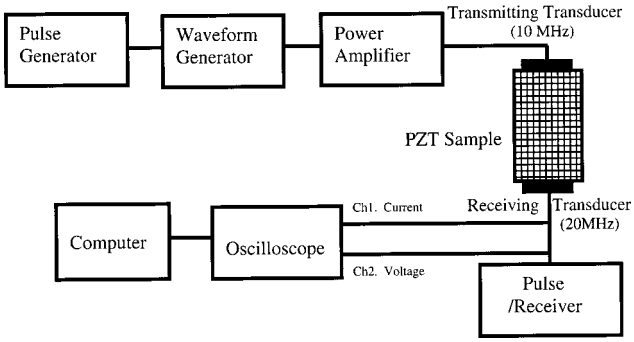

FIG. 1. Experimental setup for the second harmonic measurements.

The determination of β by the second harmonic generation technique needs to measure the absolute amplitude of the first and second harmonic waves. The existing absolute amplitude measurement methods are: (1) capacitive detector,[8] (2) contact transducer,[10] and (3) optic interferometer.[11] PZT ceramics are fairly lossy materials due to the existence of porosity. They exhibit large ultrasonic attenuation at higher frequencies.[12] On the other hand, using lower working frequencies will result in an increase of the sample size for obtaining a reasonable signal to noise ratio since the amplitude of the second harmonic wave is proportional to the propagation distance and the inverse of wavelength square. Considering all these factors, the contact transducer method was chosen for our experiments. Comparing the capacitive detector and optic interferometer, the contact transducer has higher sensitivity since a narrower band receiver was used. In our experiments, either 5 or 10 MHz is chosen as the fundamental frequency so that the corresponding second harmonic frequency is either 10 or 20 MHz. The experimental setup is schematically shown in Fig. 1. A toneburst signal from an arbitrary waveform generator (AWG 2021, Tektronix) is fed into a power amplifier (LogiMetrics). The output of the amplifier is applied to the transmit transducer (5 or 10 MHz) and the acoustic wave arriving at the end of the sample is detected by a receive transducer (10 or 20 MHz).

In order to obtain the absolute amplitude of the fundamental and second harmonic waves, the receive transducer must be calibrated. We have followed the calibration prin-

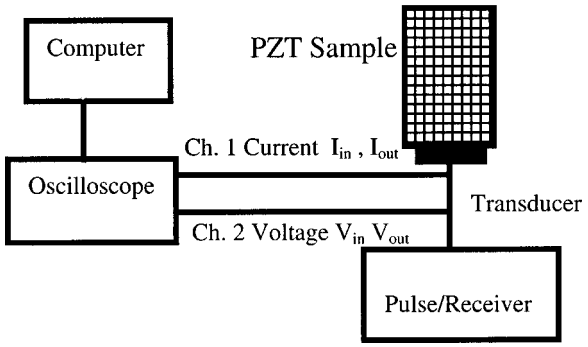

FIG. 2. Illustration of the calibration procedure of the receive transducer by the pulse-echo technique.

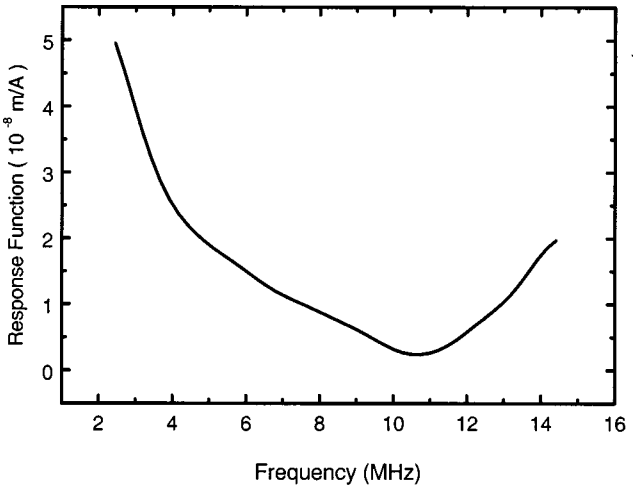

FIG. 3. Typical response function of the receive transducer.

ciple described in Ref. 10. As shown in Fig. 2, before bonding the transmit transducer to the sample, an electric pulse from a DPR35 pulser/receiver is applied to the receive transducer. Then, the current I_{in}, voltage V_{in} applied to the transducer as well as the current I_{out}, voltage V_{out} from the first back wall echo are recorded by a digital oscilloscope (Tek TDS 460 A). The data are then transferred to a PC computer where FFT of all four signals is performed. Finally, a so-called response function $H(\omega)$ of the receive transducer with surface area a is obtained,

$$|H(\omega)| = \sqrt{\frac{\left| I_{\text{in}}(\omega)\left(\frac{V_{\text{out}}(\omega)}{I_{\text{out}}(\omega)}\right) + V_{\text{in}}(\omega)\right|}{2\omega^2 \rho v a |I_{\text{out}}(\omega)|}}. \tag{15}$$

The acoustic wave amplitude can be simply calculated using the response function multiplied by the output current:

$$|A(\omega)| = |H(\omega)||I_{\text{out}}(\omega)|. \tag{16}$$

A typical response function is shown in Fig. 3. The transducer is a 36° Y cut $LiNbO_3$ disk with a diameter of 0.5″ and nominal center frequency of 10 MHz. It is bonded to the PZT samples by Salol. From the figure it is seen that the receive transducer can respond to both the fundamental and second harmonic waves. Thus, A_1 and A_2 can be measured at the same time. In our experiments, the output current from the receive transducer is recorded in the digital oscilloscope and then transferred to the computer. Through FFT of the waveform the electric current amplitudes corresponding to the fundamental and second harmonic waves are obtained and the A_1 and A_2 can be calculated using Eq. (16).

Since the $H(\omega)$ was obtained at a given electric load, during the nonlinear measurements, the DPR35 pulser/receiver with power off is connected with the receiver transducer in order to keep the electric load of the transducer unchanged from the calibration stage. The whole system is carefully checked to exclude the nonlinearities that may come from the system itself. The electric current probe used in our experiment is the Tek P6022 with a sensitivity of 1 mV/mA and has a good linear response within the range of the electric current in our experiments. We also checked the system with an aluminum test sample to obtain a value of $\beta = 5$, which is consistent with those reported in Ref. 10 ($\beta = 4.5$ and $\beta = 5.1$).

IV. EXPERIMENTAL RESULTS AND DISCUSSIONS

The ultrasonic nonlinearity parameter β and corresponding third-order elastic constants are measured for PZT-4, PZT-5A, PZT-5H, and PZT-5H HD. The size and geometry of the samples are listed in Table II.

Figure 4 gives the relation between the second harmonic amplitude A_2 and the square of the fundamental amplitude A_1^2 for one of the measurements. A good linear relation between A_2 and A_1^2 was found, which is expected from Eq. (11). From the slope of the straight line the β value can be calculated since the length and sound velocity of the sample as well as the wave frequency are known. The measured results for the four types of PZT ceramics are also listed in Table II.

TABLE II. Sample parameters and measured results for PZT-4, PZT-5A, PZT-5H HD, and PZT-5H. K_2 and K_3 correspond to different second- and third-order elastic constants as defined in Table I.

	PZT-4			PZT-5A			PZT-5H HD		PZT-5H	
Sample	Poled		Unpoled	Poled		Unpoled	Poled	Depoled	Poled	Depoled
orientation	Z cut	X cut	isotropic	Z cut	X cut	isotropic	Z cut	isotropic	Z cut	isotropic
shape	cubic[a]	cubic[a]	cubic[a]	cubic[a]	cubic[a]	cubic[a]	plate[b]	plate[b]	cylinder[c]	cylinder[c]
ρ (kg/m^3)	7600	7600	7600	7500	7500	7500	7800	7800	7500	7500
porosity	0.95	0.95	0.95	0.94	0.94	0.94	0.98	0.98	0.94	0.94
K_2[d]	14.7	13.2	13.2	14.1	11.7	11.7	17.1	13.5	13.4	10.6
β_u	7	16.4	13.4	5.7	4.8	3	3.1	10.4	14.9	17.4
β_c	7.03	19.5	16	5.1	4.5	2.9	3.2	8.3	15	18.3
K_{3u}[e]	−14.7	−25.6	−21.6	−12.3	−9.1	−7	−10.4	−18.1	−24	−21.6
K_{3c}[e]	−14.7	−29.7	−25.1	−11.4	−8.8	−6.9	−10.6	−15.3	−24.1	−22.6

[a]Sample size is 2.54 cm cube.
[b]Sample size is 2.54 cm×2.54 cm×0.64 cm.
[c]Cylinder sample with 2.54 cm diameter and thickness 1.27 cm.
[d]Unit: 10^{10} N/m^2.
[e]Unit: 10^{11} N/m^2.

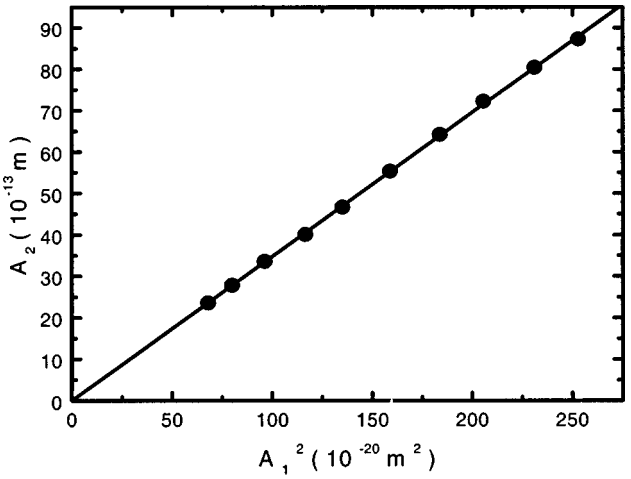

FIG. 4. Variation of the second harmonic amplitude vs the square of the fundamental amplitude.

Without taking into account the ultrasonic attenuation, the first-order approximation Eq. (7) leads to a secular solution, which states that the amplitude of the second harmonic wave will linearly increase with the wave propagation distance as indicated by Eq. (11). Obviously, this solution cannot be valid for arbitrary large amplitude of the second harmonic wave. The attenuation of PZT materials used in our experiment is fairly strong, which will reduce the amplitude of the second harmonic wave as it propagates. When both the nonlinearity and dissipation of the medium are simultaneously taken into account, it can be verified[13] that the linear accretion of the second harmonic wave with propagation distance only holds at the beginning stage of wave propagation. The general equation for the second harmonic displacement must be modified:

$$u_3^{(1)}=\frac{1}{8}\beta k^2 A_1^2 \frac{\exp[-2\alpha(\omega)z]-\exp[-\alpha(2\omega)z]}{\alpha(2\omega)-2\alpha(\omega)} \times \cos 2(\omega t-kz), \tag{17}$$

where $\alpha(\omega)$ and $\alpha(2\omega)$ are attenuation coefficients at ω and 2ω, respectively. Thus,

$$\beta=\frac{8A_2}{k^2 A_1'^2}\frac{\alpha(2\omega)-2\alpha(\omega)}{1-\exp\{-[\alpha(2\omega)-2\alpha(\omega)]L\}}, \tag{18}$$

where L is the sample length, A_1' is the attenuated fundamental amplitude measured at $z=L$. For PZT ceramics, the attenuation mainly comes from the scattering of ultrasonic wave at grain boundaries. The frequency dependence of attenuation can be obtained by using the ultrasonic spectroscopy technique.[12]

The diffraction effect associated with the finite size of the transducers also needs to be considered. If A_u and A_c are the ultrasonic wave amplitudes without and with correction of the diffraction effect, respectively, it is known that they obey the following relationship;[14]

$$A_c=A_u q^{-1}(\omega,z), \tag{19}$$

where

$$q=\{[\cos\xi-J_0(\xi)]^2+[\sin\xi-J_1(\xi)]^2\}^{1/2}, \tag{20}$$

$\xi=\omega R^2/vz$, v is the wave velocity, R is the radius of the transducer, and z is the propagation distance of ultrasonic wave,[14] which is the sample length L in our experiments.

Taking into account both the effects of attenuation and diffraction, the response function of the receive transducer becomes

$$|H_c(\omega)|=|H(\omega)|\{\exp[-\alpha(\omega)z]q(\omega,z)\}^{1/2}. \tag{21}$$

(Note: during calibration, z is twice of the sample length because the reflected echoes were used.) Then, the corrected acoustic wave amplitude is

$$A_c(\omega)=|H_c(\omega)||I(\omega)|. \tag{22}$$

In Table II, β_u and K_{3u} are the nonlinearity parameter and the K_3 value, respectively, without the attenuation and diffraction correction, while β_c and K_{3c} are the corresponding values after the correction. One can see that the corrections are not always significant due to the cancellation of the above two effects.

Although PZT ceramics contain porosity, the β values in the X_3 direction of poled PZT-4 and PZT-5A and PZT 5H HD are comparable with that of typical single crystals,[8] which agrees with the conclusion of Ref. 3. The porosity of PZT materials measured in our experiment is also listed in Table II. It was found that the poled high density PZT-5H HD has the lowest porosity of only 2%. Its nonlinearity parameter β is the smallest among all of the *Z*-cut PZT ceramics. The regular PZT-5H has 6% porosity and its β value is five times as large as that of the PZT-5H HD. Since the chemical composition of PZT 5H and PZT 5H HD are the same, it seems that more porous material also has larger nonlinearity. As pointed out by Donskoy *et al.* that the β values of some porous materials, such as rocks, could be as large as 10^3-10^4 (Ref. 15) compared to the β values of single crystals in the range of 2–14.[8]

On the other hand, different dopants in PZT ceramics definitely have strong influence to the nonlinearity, which can be seen from the β value of the PZT-4 and PZT-5A ceramics. Although PZT-5A is more porous, its β value in the X_3 direction is smaller than PZT-4, which also has much stronger nonlinearity in the X_1 direction of poled and unpoled samples.

For PZT-4 and PZT-5A we found that the sound velocity in the X_1 direction of a poled sample is the same as that of an unpoled sample (isotropic). But the nonlinearity parameter β of an unpoled sample is a little less than the β value in the X_1 direction of a corresponding poled sample. This is to say that the polarization process does not influence the linear properties of the material in the X_1 direction but the nonlinear properties have noticeable change from the poling process. This is indirect proof that that the poling process seems to generate some degree of mechanical damage in the sample due to the switching of domains.

In order to further investigate the influence of the poling process to the nonlinearity parameter, the originally poled PZT-5H HD and regular PZT-5H samples were thermally depoled. The measured nonlinearity parameters for the depoled samples are also listed in Table II. It was observed that the depoled samples have the same ultrasonic velocity as that

of the velocity along the X_1 direction of the poled samples (the same as that of unpoled samples). However, as shown in Table II, the nonlinearity parameter of the depoled samples increased about three times compared to the poled samples for PZT-5H HD. This means that the depoling process also creates microstructural changes in the ceramic. It further reveals the fact that the nonlinear parameters are much more sensitive to microstructural changes than the linear parameters. Specifically, we may use the nonlinearity parameter to distinguish an unpoled sample from a depoled sample for the PZT-5H HD. The same trend was also observed in the regular PZT-5H ceramic, but it is far less drastic than what occurred in PZT-5H HD. This may be understood by the fact that the regular PZT-5H already contains much higher porosity and the depoling process does not create significant change to its porous structure.

V. SUMMARY AND CONCLUSIONS

The nonlinear properties of lead zirconate–titanate piezoceramics PZT-4, PZT-5A, PZT-5H and PZT-5H HD have been investigated by means of the ultrasonic second harmonic generation method. In the X_1 direction, the ultrasonic nonlinearity parameter β represents solely the elastic nonlinearity associated with c_{111}, but in the piezoelectric stiffened direction (X_3 direction), the contributions of piezoelectric and dielectric nonlinearities are also included in the ultrasonic nonlinearity parameter β. Therefore, only the effective third-order elastic constant c^D_{333} can be determined.

Due to different porosities and different dopants in these PZT ceramics, the observed nonlinearity parameter β covers a wide range from 3 to 19. For poled PZT ceramics, the β values in the X_3 direction are comparable to that of other single crystals, but the nonlinearity in the X_1 direction is higher than the typical value for single crystals. An important finding from our study is that the nonlinearity parameter is much more sensitive to internal structural changes than the linear parameters. We could use the nonlinearity parameter to discriminate unpoled and depoled PZT samples because the poling and depoling process both cause damages to the microstructure inside the ceramics,[16] which are invisible to linear effects.

ACKNOWLEDGMENT

The research was sponsored by the NIH under Grant No. P41 RR 11795-010A and the ONR MURI Grant No. N00014-96-1-1173.

[1] Y. Cho and K. Yamanouchi, J. Appl. Phys. **61**, 1728 (1987).
[2] H. Beige, Ferroelectrics **51**, 113 (1983).
[3] J. K. Na and M. A. Breazeale, J. Acoust. Soc. Am. **95**, 3213 (1994).
[4] Neil W. Ashcroft and N. David Mermin, in *Solid State Physics* (Saunders College, Philadelphia, PA, 1976).
[5] D. H. McMahon, J. Acoust. Soc. Am. **44**, 1007 (1968).
[6] D. F. Nelson, in *Electric, Optic and Acoustic Interactions in Dielectrics* (Wiley, New York, 1979).
[7] B. A. Auld, in *Acoustic Fields and Waves in Solids* (Wiley, New York, 1973).
[8] M. A. Breazeale and J. Philip, in *Physical Acoustics* edited by W. P. Mason (Academic, New York, 1984), Vol. XVII, pp. 1–60.
[9] J. F. Nye, in *Physical Properties of Crystals* (Clarendon, Oxford, 1985).
[10] G. E. Dace, R. B. Thompson, L. J. H. Brasche, D. K. Rehbein, and O. Buck, in *Review of Progress in Quantitative Nondestructive Evaluation*, edited by D. O. Thompson and D. E. Chimenti (Plenum, New York, 1991), Vol. 10B, p. 1685.
[11] A. Moreau, J. Acoust. Soc. Am. **98**, 2745 (1995).
[12] H. Wang, W. Jiang, and W. Cao, J. Appl. Phys. **85**, 8083 (1999).
[13] B. T. Beyer, in *Nonlinear Acoustic*, Naval Sea System Command, 1974.
[14] W. Cao, G. Barch, W. Jiang, and M. A. Breazeale, Phys. Rev. B **38**, 10244 (1988).
[15] D. M. Donsky, K. Khashanah, and T. G. McKee, Jr., J. Acoust. Soc. Am. **102**, 2521 (1997).
[16] E. C. Subbarao, V. Srikanth, W. Cao, and L. E. Cross, Ferroelectrics **145**, 271 (1993).